NUMERICAL THREE-DIMENSIONAL ANALYSIS OF THE MECHANISM OF FLOW AND HEAT TRANSFER IN A VORTEX TUBE

by

Alireza HOSSEIN NEZHAD and Rahim SHAMSODDINI

Original scientific paper
UDC: 532.52/.54:536.24:66.011
DOI: 10.2298/TSCI0904183N

A fully three-dimensional computational fluid dynamic model is used to analyse the mechanism of flow and heat transfer in a vortex tube. Vortex tube is a simple circular tube with interesting function and several industrial applications and contains one or more inlets and two outlets. It is used as a spot cooling device in industry. The past numerical investigations of vortex tube have been performed with the two-dimensional axisymmetric assumption but in the present work this problem is studied fully three-dimensional without making that assumption. Using this model, appropriate numerical results are presented to clarify physical understanding of the flow and energy separation inside the vortex tube. It is observed that there are considerable differences between the results of the two aforementioned models, and that the results of fully three-dimensional model are more accurate and agree better with available experimental data. Moreover, the parameters affecting the cooling efficiency of the vortex tube are discussed.

Key words: *vortex tube, two nozzles, numerical, fully three-dimensional*

Introduction

Vortex tube first was discovered by Ranque in 1933 when he was a student of physics. When he was studying on a pump, he accidentally noticed that the air that enters tangentially into a pipe exits form one outlet at a lower temperature and from the other outlet at a higher temperature than the inlet flow temperature. The observation of this matter caused Ranque to abandon his studies on pump and begin investigations on the vortex tube [1]. But his research did no reach to a conclusion and later Hilsh revised Ranque's findings and improved the efficiency of a vortex tube. Moreover, Hilsh presented the first concept about the efficiency of the vortex tube. He explained that temperature separation occurs because radial gradient of tangential velocity results in frictional coupling between different layers of rotating flow which leads to energy transfer from inner layers to outer layers via shear work [2]. Vortex tube is a simple and useful device without any moving parts, electrical or chemical power input and special equipments. It is capable of producing air with desired cold or hot temperature and low cost. It is currently considered for commercial low temperature applications such as cooling of electronic pieces, testing of thermal sensors, cooling of controlling cabins, local heating of enclosures, cooling of cutting tools and cooling of spots under thermal stresses [3, 4]. Other applications of vortex tube include extensive uses in fast starting up of the steam power stations, liquefying natural gas, nuclear reactors, gas separations, and cooling the laboratories used to maintain materials in low temperature. Two types of vortex tube used in industry are parallel and counter flow, and be-

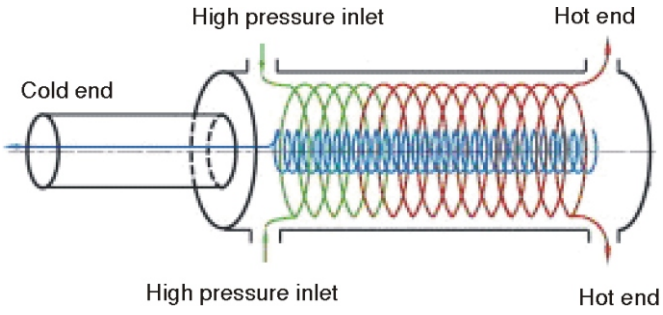

Figure 1. Vortex tube, hot and cold streams, cold and hot outlets and flow inlets [5]

cause of wide applications of the latter, it is studied in the present work. In a vortex tube compressed air enters tangentially into it through one or more nozzles. Part of the flow rotationally passes alongside the wall and exits as hotter fluid from the hot end and the other part comes back from the hot end alongside the axis to the cold end and exits as colder flow. Geometry of the vortex tube including flow inlets, cold and hot outlets and associated flows including cold and hot streams are shown in fig. 1.

About the reasons of the formation of two vortex flows inside the vortex tube, several theories have been presented but two of them have been more acceptable. According to the first theory, radial gradient of the tangential velocity results in friction coupling between different layers which leads to the transfer of energy from the inner layers to the outer layers via the shear work. The second theory explains thermodynamically this phenomenon and states that a free expansion inside the vortex tube is the reason for the formation of two vortex flows inside the tube. From the thermodynamical view, it is impossible a flow can be separated into two part, one with higher energy and the other with lower energy than that of the main flow energy in a constant pressure process. Thus, a concept that may explain this phenomenon is that flow should expand adiabatically at the end of the tube away from the nozzles from high pressure to low pressure [6]. Using computational fluid dynamics (CFD) some investigators have been able to explain the function of vortex tube reasonably: Frohlingsdorf *et al.* by using computational code based on CFX (a commercial computational fluid dynamics software) along with k-ε model investigated the mechanism of energy separation inside the vortex tube [7]. Eiamsa *et al.* by employing algebraic stress model (ASM) studied vortex tube and claimed that ASM model analysis vortex tube more accurately [3]. Behera *et al*. studied the effects of nozzle numbers on the energy separation inside the vortex tube using CFD and employing experiments [8]. Aljuwayhel *et al*. studied the mechanism of flow and energy separation inside the vortex tube using renormalization group (RNG) k-ε and standard k-ε models. They used a two-dimensional axisymmetric model along with the effects of the rotational velocity and reported that RNG k-ε model predicts better the function of the vortex tube [4]. Skye *et al.* did a similar work to the work of Aljuwayhel, but claimed that satandard k-ε model predict the performance of the vortex tube better than RNG k-ε model [9]. Farouk *et al*. used large eddy simulation and analysed flow filed and temperature separation comparatively accurate [5]. Eiamsa-ard *et al*. experimentally studied the effect of the nozzle numbers on the performance of a vortex tube [10]. Hartnett *et al*. experimentally studied the velocity, temperature, and pressure distributions inside a uni-flow vortex tube [11]. More references can be found in [12] in which Eiamsa-ard *et al*. reviewed extensively Ranque-Hilsch effects in vortex tubes.

Two-dimensional axisymmetric model has been used in the most of the models mentioned above. The axisymmetric model ignores the effects of nozzles arrangements around the vortex tube, but the three-dimensional model takes into account those effects. In this paper using a three-dimensional model and considering the effects of the nozzles, we analyse a vortex tube with two nozzles. For this purpose, we compare the results of three-dimensional model with the results of two-dimensional model and available experimental data.

Mathematical formulation

Flow is assumed compressible and turbulent and governing equations for fluid flow and heat transfer are:

– continuity equation:

$$\frac{\partial}{\partial x_{\mathrm{i}}}(\rho u_{\mathrm{i}}) \quad 0 \tag{1}$$

– momentum equations:

$$\frac{\partial}{\partial x_j}(\rho u_i u_j) \qquad \frac{\partial p}{\partial x_i} \quad \frac{\partial}{\partial x_j} \mu \frac{\partial u_i}{\partial x_j} \quad \frac{\partial u_j}{\partial x_i} \quad \frac{2}{3}\delta_{ij} \frac{\partial u_{\mathrm{k}}}{\partial x_{\mathrm{k}}} \qquad \frac{\partial}{\partial x_j}(\overline{\rho u_i u_j}) \tag{2}$$

– energy equation:

$$\frac{\partial}{\partial x_i} u_i \rho \quad h \quad \frac{1}{2} u_j u_j \qquad \frac{\partial}{\partial x_j} k_{\mathrm{eff}} \frac{\partial T}{\partial x_j} \quad u_i (\tau_{ij})_{\mathrm{eff}} \ , \quad k_{\mathrm{eff}} \quad K \quad \frac{c_{\mathrm{p}} \mu_{\mathrm{t}}}{\mathrm{Pr}_{\mathrm{t}}} \tag{3}$$

In the above equations ρ [kgm^{-3}] denotes the density, u_i[ms^{-1}] – the mass-averaged velocity component in the direction of Cartesian coordinate i, i = 1, 2, 3 Cartesian coordinate directions, μ [kgm^{-1}s^{-1}] – the viscosity, p [Pa] – the pressure, d_{ij} is the Kronecker delta, u_{i} [ms^{-1}] – the fluctuating component of velocity, K [Wm^{-1}K^{-1}] – the conductivity coefficient, μ_{t} [kgm^{-1}s^{-1}] – the turbulent viscosity, Pr_{t} – the turbulent Prandtl number, T [K] – the mass-averaged temperature, $(\tau_{ij})_{\mathrm{eff}}$ – the effective stress tensor, and h [Jkg^{-1}] is the mass-averaged enthalpy.

The first term on the left hand side of the energy equation represents the rate of total energy of the fluid element lost by convection; the first term on the right-hand side of it represents energy transfer due to conduction; and the term involving $(\tau_{ij})_{\mathrm{eff}}$ represents the viscous dissipation. It is noted that summation rule is used for repeated indices: i and j.

State equation for an ideal gas:

$$p = \rho R T \tag{4}$$

where R is specific constant of an ideal gas.

Using k-ε model, Reynolds's stresses appeared on the right hand side of eq. (2) and effective stress tensor are substituted by the equations:

$$\overline{\rho u_i u_j} \quad \mu_t \frac{\partial u_i}{\partial x_j} \quad \frac{\partial u_j}{\partial x_i} \quad \frac{2}{3} \rho k \quad \mu_{\mathrm{t}} \frac{\partial u_{\mathrm{k}}}{\partial x_{\mathrm{k}}} \quad \delta_{ij} \tag{5}$$

$$(\tau_{ij})_{\mathrm{eff}} \quad \mu_{\mathrm{eff}} \frac{\partial u_j}{\partial x_i} \quad \frac{\partial u_i}{\partial x_j} \qquad \frac{2}{3} \mu_{\mathrm{eff}} \frac{\partial u_{\mathrm{k}}}{\partial x_{\mathrm{k}}} \delta_{ij} \tag{6}$$

where k [m^{2}s^{-2}] is the turbulent kinetic energy, and μ_{eff} [kgm^{-1}s^{-1}] – the effective viscosity. Using RNG model, ε and k satisfy the following two equations:

$$\frac{\partial}{\partial x_i}(\rho k u_i) \qquad [\alpha_k \mu_{\mathrm{eff}} \quad k] \quad 2\mu_{\mathrm{t}} E_{ij} E_{ij} \quad \rho\varepsilon \tag{7}$$

$$\frac{\partial}{\partial x_i}(\rho \varepsilon u_i) \qquad [\alpha_\varepsilon \mu_{\mathrm{eff}} \quad \varepsilon] \quad C_{1\varepsilon}^* \frac{\varepsilon}{k} 2\mu_{\mathrm{t}} E_{ij} E_{ij} \quad C_{2\varepsilon} \rho \frac{\varepsilon^2}{k} \tag{8}$$

where the constant and variable parameters used in the above equations are:

$$\mu_{\text{eff}} = \mu + \mu_{\text{t}} \tag{9}$$

$$C_{1\varepsilon}^{*} \quad C_{1\varepsilon} \quad \frac{\eta \left(1 - \frac{\eta}{\eta_0}\right)}{1 + \beta\eta^3} \tag{10}$$

$$\eta \quad \sqrt{2E_{ij}E_{ij}}\,\frac{k}{\varepsilon} \tag{11}$$

$$E_{ij} \quad \frac{\partial U_i}{\partial x_j} \quad \frac{\partial U_j}{\partial x_i} \tag{12}$$

$C_\mu = 0.0845$, $\alpha_{\text{k}} = \alpha_\varepsilon = 1.39$, $C_{1\varepsilon} = 1.44$, $C_{2\varepsilon} = 1.92$, $\text{Pr}_{\text{t}} = 0.85$, $\eta_0 = 4.377$, $\beta = 0.012$

In the above equations E_{ij} is the tensor of strain rate, ε [m^2s^{-3}] – the rate of turbulece dissipation energy, α_{k} and α_ε are inverse of Prandtl number corresponding, respectively, with equations of k and ε, Pr_{t} is the turbulent Prandtl number, and η_0, β, C_μ, $C_{1\varepsilon}$, $C_{2\varepsilon}$, $C_{1\varepsilon}^{*}$, η, and C_υ are constants of k-ε model. In RNG k-ε model effective viscosity, μ_{eff}, is calculated by using formula:

$$\text{d} \quad \frac{\rho^2 k}{\sqrt{\varepsilon\mu}} \quad 1.72\frac{\hat{\upsilon}}{\sqrt{\hat{\upsilon}^3 \quad 1 \quad C_\upsilon}}\text{d}\hat{\upsilon}, \quad \hat{\upsilon} \quad \frac{\mu_{\text{eff}}}{\mu}, \quad C_\upsilon \quad 100 \tag{13}$$

To solve the turbulent flow in the vortex tube RNG k-ε model is used according to following reasons:

– the RNG model has an additional term in its ε equation that significantly improves the accuracy for rapidly strained flows,
– the effect of swirl on turbulence is included in the RNG model, enhancing accuracy for swirling flows,
– the RNG theory provides an analytical formula for turbulent Prandtl numbers, while the standard k-ε model uses user-specified constant values, and
– while the standard k-ε model is a high-Reynolds-number model, the RNG theory provides an analytically-derived differential formula for effective viscosity that accounts for low-Reynolds-number effects. Effective use of this feature does, however, depend on an appropriate treatment of the near-wall region.

Geometry and boundary conditions

The mechanism of flow and heat transfer in a vortex tube of the Hilsh-Ranque type is investigated. Its diameter is 1 cm, its length is 10 cm and the other dimensions are shown schematically in fig. 2, with axisymmetric assumption.

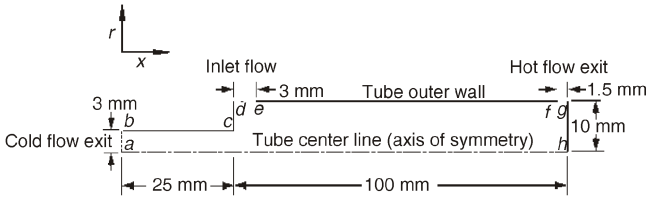

Figure 2. Axisymmetric representation of geometry of Hilsh-Ranque vortex tube

A three-dimensional representation of a vortex tube with two nozzles and other dimensions similar to that of fig. 2 is shown in fig. 3.

Number of nozzles used in a vortex tube can be two, four or even more. As it is shown in fig. 3, nozzles can be connected with an angle with tangential direction so that flow leaving them has appropriate tangential velocity component.

A conic valve is used as discharge valve at the hot outlet to adjust the hot flow rate, outlet pressure, and temperature. The outlet parameters control cold temperature and cold mass flow rate. Thus by adjusting the hot conic valve, the hot and cold temperature are adjusted. For simplicity in the present three-dimensional computation the conic valve at the exit is replaced with radial outlet as shown in the hot end in fig. 3.

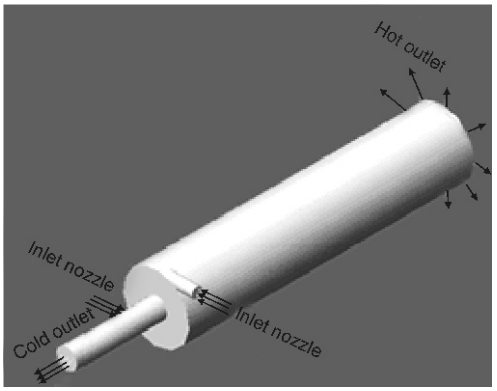

Figure 3. Geometry of the three-dimensional vortex tube

Boundary conditions and numerical procedure

Boundary conditions in the vortex tube are:

(1) at the nozzles inlets, compressed air with known mass flow rate or pressure and total temperature is assumed,
(2) at the hot and cold outlet, pressure is assumed, and
(3) the wall of the vortex tube is assumed insulated and no slip conditions are used for flow velocity components.

Experimental data have been used to determine the numerical values of the boundary conditions at the nozzle inlets and cold and hot outlets [8, 9].

According to the three-dimensional geometry shown in fig. 4, finite volume method with a three-dimensional mesh is used and the boundary conditions are applied. Air is used as an ideal gas and the flow is assumed compressible. Quick scheme is used to discretize convective terms, and coupled procedure is used to solve the momentum and energy equations simultaneously. To model the Reynolds stresses, RNG k-ε model is employed.

In order to show grid independency of the results, four cases of grids shown in fig. 4 and 5 are studied: $N = 20000$ nodes, $N = 40000$ nodes, $N = 80000$ nodes, and $N = 120000$ nodes.

Since the problem is three-dimensional, according to the complexity of the equations and meshes we have assumed the convergence error for all of the equations be as 0.0001. Also the balance of the inlet and outlet masses is used as a convergence condition. Variation of the hot outlet pressure and flow rate can have significant influence on the performance of vortex tube and cold outlet flow conditions.

Using aforementioned four cases of grids, in fig. 6 variation of temperature on the axis of the vortex tube for the case p_h =

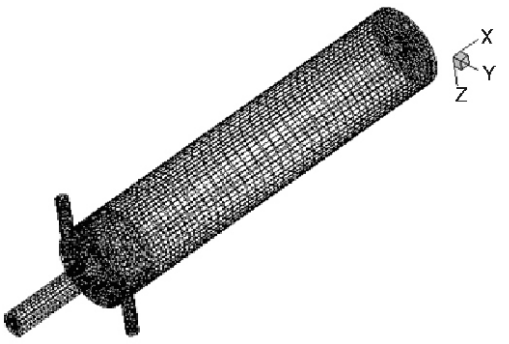

Figure 4. Three-dimensional grid of the vortex tube

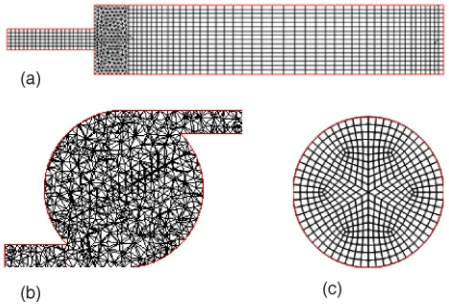

Figure 5. (a) Gird viewed on the plane passing through the axis (plane $y = 0$); (b) grids viewed on the cross-section cutting the inlet nozzles; (c) grid viewed on the middle cross-section of the vortex tube

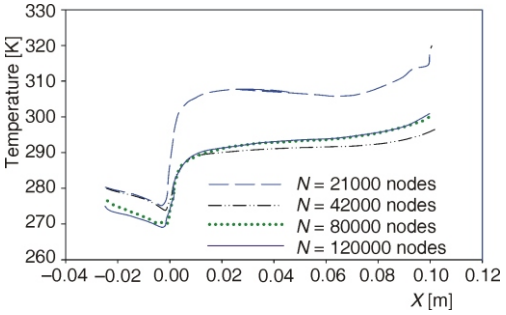

Figure 6. Grid effect on the variation of temperature on the axis of a vortex tube for the case p_h = 180 kPa, $\dot{m}$ = 8.35 g/s, T_{oin} = 300 K, and p_c = 103 kPa

= 180 kPa, $\dot{m}_i$ = 8.35 g/s, T_{oin} = 300 K, and p_c = 103 kPa in which p_h is the hot end pressure, T_{oin} – the total temperature of nozzles inlet, $\dot{m}_i$ – the mass folw rate flows into the vortex tube through the nozzles inlets, and p_c – the cold end pressure, has been plotted. It is observed that a grid with N = 80000 nodes is enough to give reliable and grid independent results.

Results and discussions

Figures 7 and 8 shows temperature and pressure contours, respectively, on the plane passing through the axis of the vortex tube (plane $y = 0$) for the case with p_h=180 kPa, for $\dot{m}_i$ =

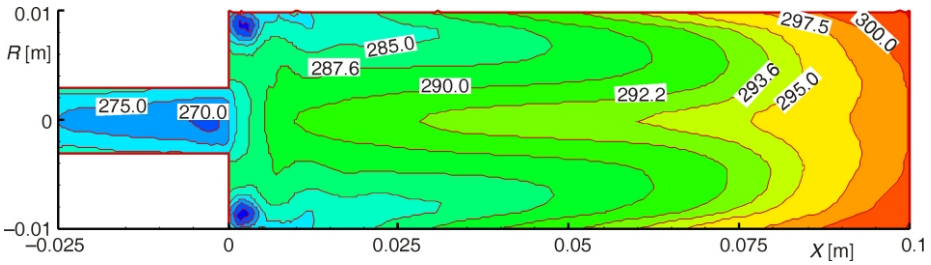

Figure 7. Temperature contours on the plane passing through the axis (plane $y = 0$) for the case p_h = 180 kPa, p_c = 103 kPa, $\dot{m}$ = 8.35 g/s, and T_{oin} = 300 K (color image see on our web site)

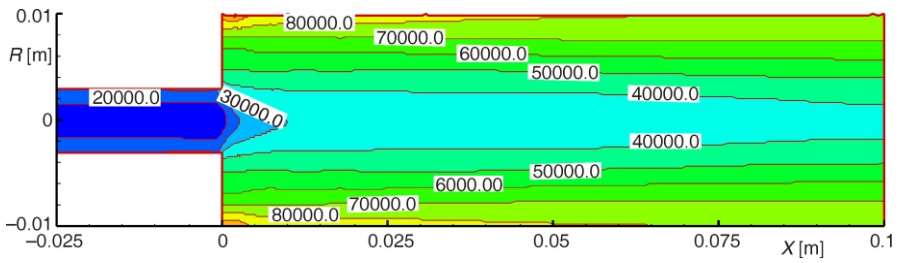

Figure 8. Pressure contours on the plane passing through the axis (plane $y = 0$) for the case p_h = 180 kPa, p_c = 103 kPa, $\dot{m}$ = 8.35 g/s, and T_{oin} = 300 K (color image see on our web site)

= 8.35 g/s and p_c = 103 kPa. It is observed that the cold outlet temperature is about 0 °C and hot outlet temperature is about 33 °C, and temperature decreases gradually from hot end to the cold end.

Figure 8 shows that pressure decreases gradually toward the center of the vortex tube. In other words, expansion occurs which causes temperature drop toward the center of the vortex tube.

Analysis of the mechanism of flow and energy separation

To analyse the mechanism of flow and energy separation, contours of axial velocity and streamlines are drawn in figs. 9 and 10, respectively, on the plane passing through the axis (plane $y = 0$) for the case $\dot{m}_{in}$ = 8.35 g/s, T_{oin} = 300 K, p_h = 180 kPa, and p_c = 103 kPa. Figure 9 shows that streamlines next to the wall bend toward the hot outlet, while stream lines alongside the axis turn toward the cold outlet. In addition, two almost symmetric vortices are formed near the cold end of the vortex tube. Figure 10 shows that the sign of the axial velocity next to the wall is positive which means flow is toward hot end and as approaching to the center its sign changes to negative indicating that flow is toward cold end. The line with zero sign makes the separation line for flow and energy.

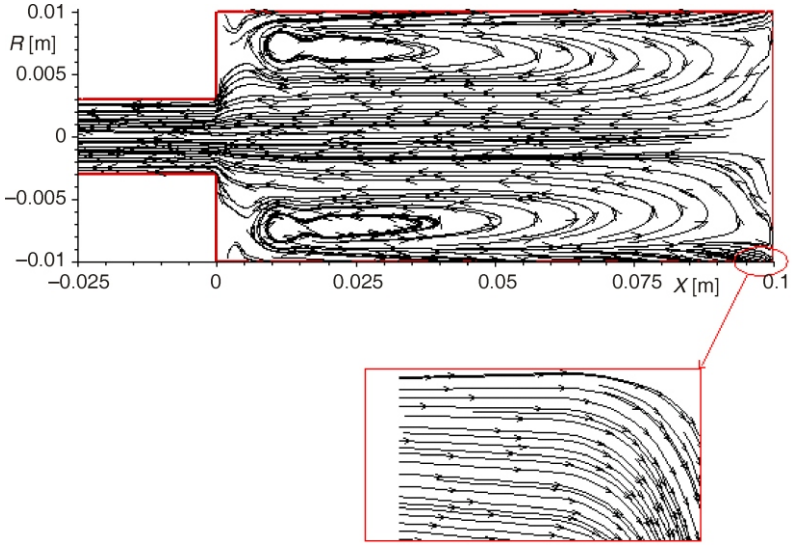

Figure 9. Streamlines on plane passing through the axis (plane $y = 0$) of the vortex tube

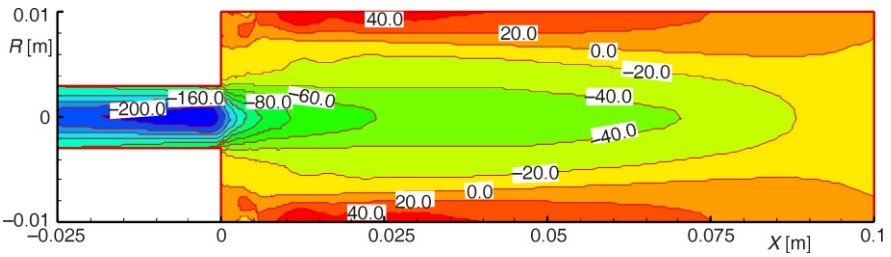

Figure 10. Contours of axial velocity on a plane passing through the axis (plane $y = 0$) of the vortex tube (color image see on our web site)

One of the advantages of three-dimensional analysis is that the flow inside the nozzles can be investigated. To complete the analysis of the mechanism of flow separation, streamlines on the cross-section including nozzles are shown in the left side of fig. 11. It is observed that the streamlines leaving the nozzles and entering the vortex tube do not go further specified radius. These streamlines are related to the hot flow from the cold end to the hot end of the vortex tube. The remaining streamlines drawn in the right side of fig. 11 show that they do not contain any streamline originated from the nozzles. These streamlines are related to the cold flow from the hot end to the cold end along side the axis of the vortex tube. Thus these two streamlines also confirm the separation of flow and energy.

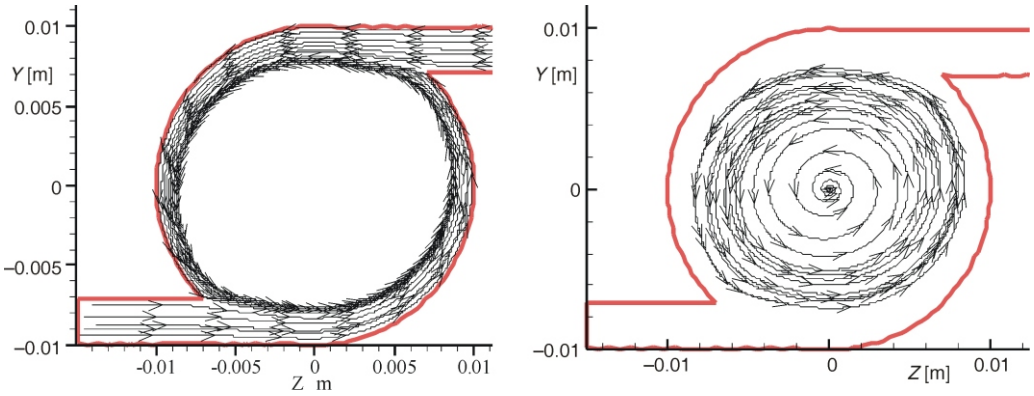

Figure 11. Stream lines located on the cross-section and containing the nozzles: (left) leaving the nozzles, and (right) not originated from the nozzles for the case $\dot{m}$ = 8.35 g/s, T_{oin} = 300 K, p_h = 180 kPa, and p_c = 103 kPa

In fig. 12 contours of velocity on a plane passing through the axis (plane $y = 0$) of the vortex tube for the case $\dot{m}_{in}$ = 8.35 g/s, T_{oin} = 300 K, p_h = 180 kPa, and p_c =103 kPa are shown. According to figs. 8 and 12, it is observed that the high pressure outer layers, near to the walls of

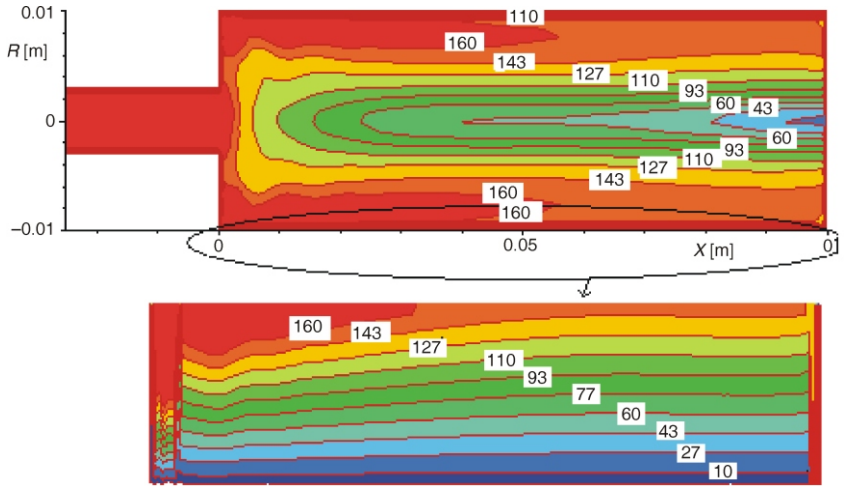

Figure 12. Contours of velocity on a plane passing through the axis (plane $y = 0$) of the vortex tube (color image see on our web site)

the vortex tube, have low velocities while the low pressure inner layers, near the axis, have large velocities and hence a larger kinetic energy. This kinetic energy change contributes to reduce the temperature of the region with higher kinetic energy, or core region. In fig. 13 contours of the tangential velocity on the mid-cross-section perpendicular to the axis of the vortex tube for the same case of fig. 12 are shown. It is observed that the tangential velocity decreases radially in the low velocity region near the wall. This tangential velocity gradient will lead to the transfer of shear work from the core region, with higher tangential velocity, to the outer region, with lower tangential velocity, resulting lower temperature in the core region. It is concluded that these two factors contribute significantly in generating energy separation in the vortex tube.

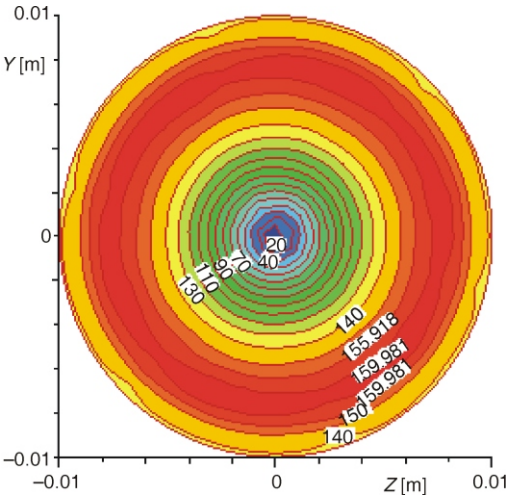

Figure 13. Contours of tangential velocity on the mid-cross-section perpendicular to the axis of the vortex tube (color image see on our web site)

Comparison between present three-dimensional and axisymmetric and previous two-dimensional axisymmetric studies

All of the contours drawn on the plane crossing the vortex tube and including the axis (plane $y = 0$) confirm the accuracy of two-dimensional axisymmetric assumption. But the contours drawn on the cross-section including the nozzles for the case $\dot{m}_{in} = 8.35$ g/s, $T_{oin} = 300$ K, $p_h = 180$ kPa, and $p_c = 103$ kPa as shown in fig. 14 indicates that the results are not axisymmetric. On the other hand the pressure contours on a cross-section at the middle of the vortex tube for the same case in fig. 15, confirms the axisymmetric assumption. We conclude that as we move away from the end containing nozzles toward the other end of the vortex tube the flow becomes more axisymmetric. Therefore, three-dimensional analysis of the vortex tube gives more accurate results compare to two-dimensional axisymmetric analysis.

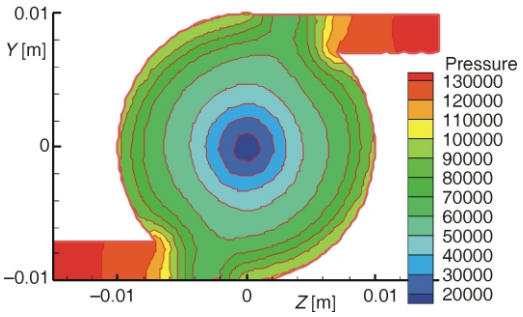

Figure 14. Gauge pressure contour located on the nozzle end cross-section perpendicular to the axis of the vortex tube (color image see on our web site)

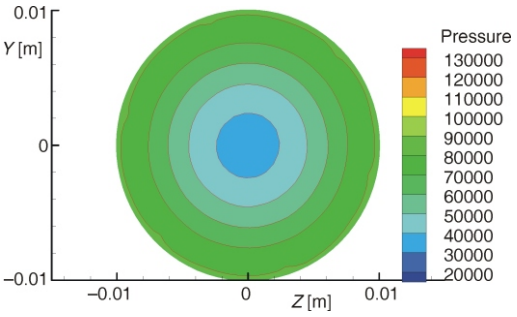

Figure 15. Gauge pressure contour located on the mid-cross-section perpendicular to the axis of the vortex tube (color image see on our web site)

In fig. 16 temperature contours of three numerical solutions on the plane crossing the vortex tube and containing the axis for the case $p_{in} = 300$ kPa, $T_{oin} = 300$ K, $p_h = 156$ kPa, and $p_c = 101$ kPa are presented: (a) axisymmetric solution of ref. [13], (b) axisymmetric solution of the present work, and (c) three-dimensional solution of the present work. It is observed that ref. [13] predicts temperature 2 °C lower than the temperature of the three-dimensional solution of the present work in the cold region. Moreover, the difference between temperature contours in the region near the nozzles is clearly observed.

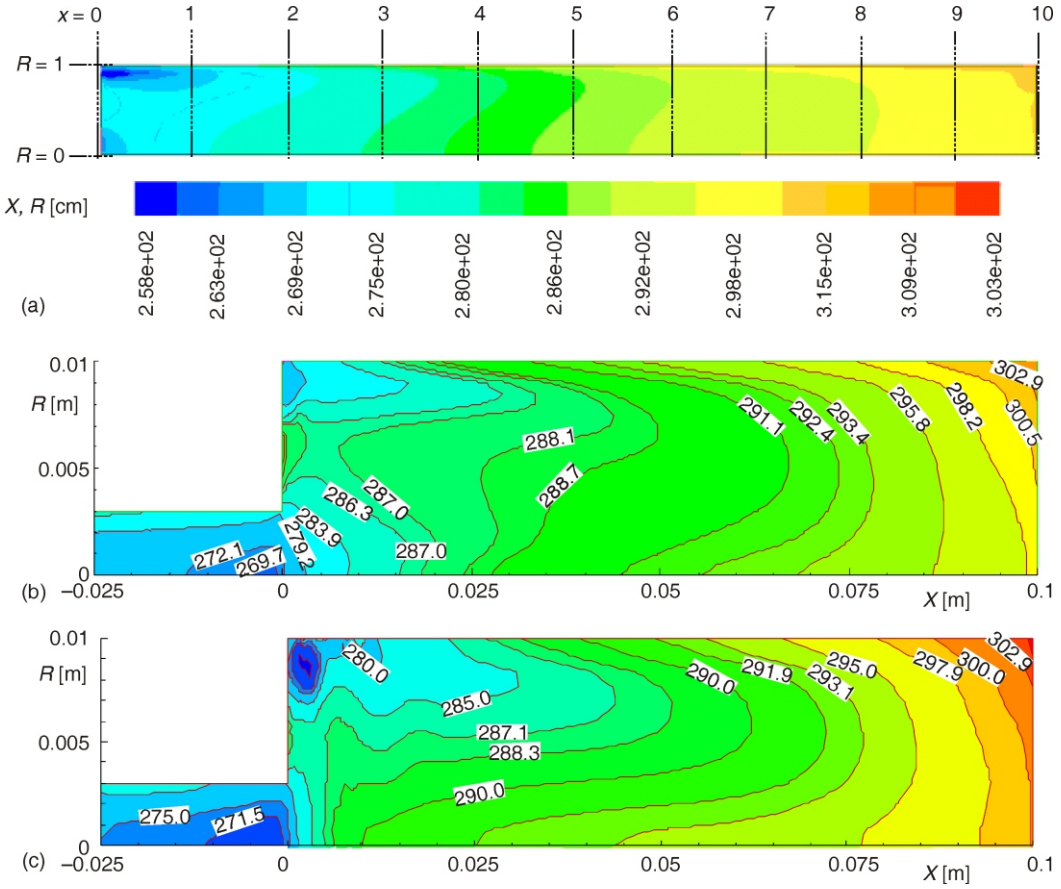

Figure 16. Temperature contours on the plane crossing the vortex tube and including the axis: (a) ref. [13], (b) axisymmetric solution of the present work, and (c) three-dimensional solution of the present work at plane $y = 0$ (color image see on our web site)

Figure 17 shows the streamline obtained form axisymmetric solution of ref. [4] and three-dimensional solution of the present work on the plane crossing longitudinally vortex tube at (plane $y = 0$) and including its axis. Agreement between two solutions is observed in the region away from the nozzles but differences exist in the region near the nozzles. The three-dimensional solution takes into account the effects of the nozzles while two-dimensional solution ignores their effect.

In figs. 16 and 17 the results was compared qualitatively. To compare quantitatively in fig. 18 total temperature *vs*. radial distance obtained from axisymmetric solution of ref. [13] and axisymmetric solution of the present work in different axial locations are drawn on the plane crossing longitudinally vortex tube and including its axis for the case $P_{in} = 300$ kPa and $T_{oin} =$ = 300 K. The results show maximum 0.07% difference between these two solutions.

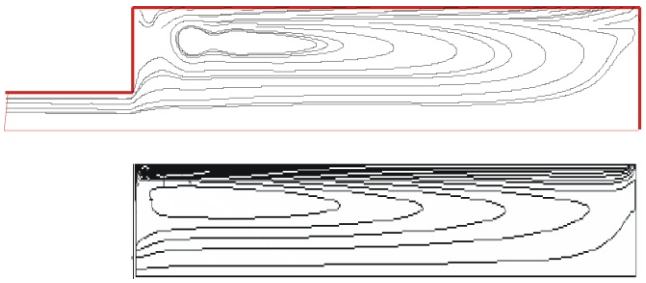

Figure 17. streamlines on the plane crossing the vortex tube and including the axis for the case pin 300 kPa T_{oin} =300K, p_h = 156 kPa and p_c =101 kPa Top: three dimensional solution of the present work, bottom: ref. [4]

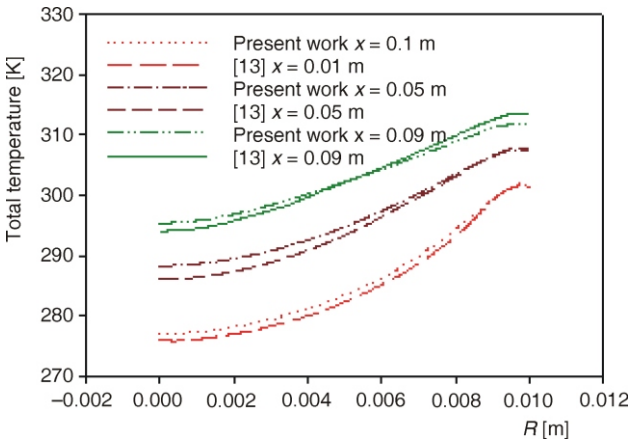

Figure 18. Comparison of the variation of total temperature *vs*. radial distance at different axial locations from the inlet on the plane crossing longitudinally vortex tube and including its axis for the case p_{in} = 300 kPa, T_{oin} = 300 K, p_h = 156 kPa, and p_c = 101 kPa between ref. [13] and present axisymmetric work

Variation of ΔT_c, difference between inlet nozzle temperature and cold end, *vs*. μ_c, cold mass fraction, of the present two- and three-dimensional solution with two nozzles is compared with ref. [10] in fig. 19. The comparison shows maximum 19.9% difference between present three-dimensional numerical work and experimental result of ref. [10]. The comparison for the present two-dimensional numerical work shows 40% difference which indicates that axisymmetric model overestimates ΔT_c in comparison with three-dimensional model.

Non-dimensional analysis

Assuming constant geometry and using non-dimensional analysis three non-dimensional parameters which include ratio of hot outlet pressure to cold outlet pressure, ratio of hot outlet total temperature to cold outlet total temperature, and ratio of cold outlet mass flow rate to inlet mass flow rate are achieved. The results are shown according to these non-dimensional parameters and discussed.

Figure 20 shows the variation of total temperature ratios versus cold mass fraction for the present axisymmetric and three-dimensional numerical solutions. It is observed that there is large difference between the present axisymmetric and three-dimensional numerical solutions.

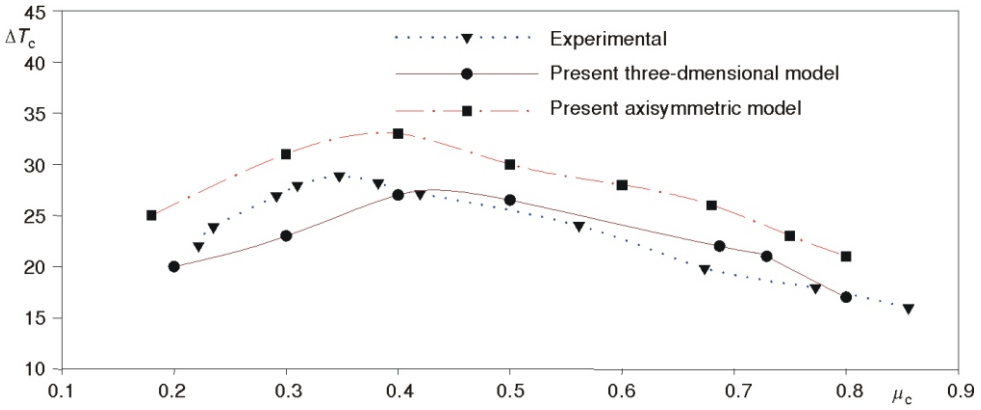

Figure 19. Comparison of the variation of ΔT_c, difference between inlet nozzle temperature and cold end, vs. μ_c cold mass fraction, of the present three-dimensional and axisymmetric solution with two nozzles with results of ref. [10]

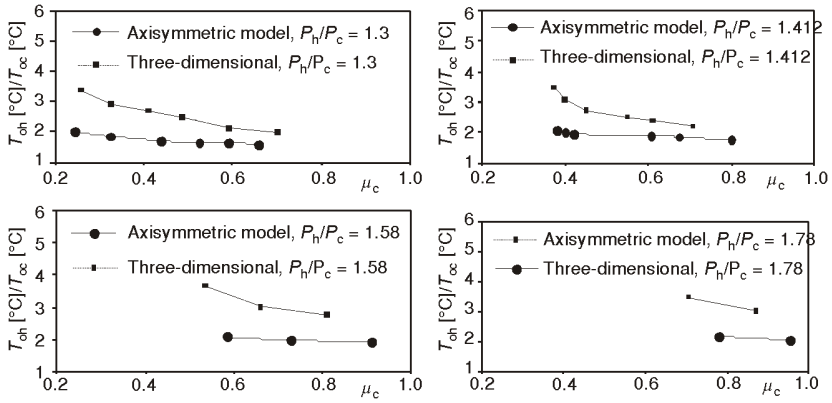

Figure 20. Variation of total temperature ratios *vs.* cold mass fraction for the present axisymmetric numerical solution for the two nozzle vortex tube for the case $\dot{m}$ = 8.35 g/s, and T_{oin} = 300 K

This results leads to the conclusion that analysing the two nozzles vortex tube with three-dimensional model gives more accurate result than two-dimensional axisymmetric model. We see that as the ratio of hot end to cold end pressure increases, the range of the ratio of the cold to hot mass flow rate reduces. The reason is that increasing the hot to cold pressure ratio is equivalent to more closing the hot end valve, which leads to reducing the hot mass flow rate and thus increasing μ_c.

Drawing some important dimensional quantities help us to understand physics of the problem. According to this fact in fig. 21 variation of cold temperature *vs*. cold mass flow rate in different pressure ratios for axisymmetric and three-dimensional solutions has been plotted. It is observed that cold outlet temperature increases with cold mass flow rate. Moreover, there is maximum 75% difference between the result of axisymmetric and three-dimensional solutions.

Also It is seen that with the increase of pressure ratio, lower cold outlet temperature can be achieved.

From the results of fig. 21 variation of power of cooling *vs*. cold temperature in different pressure ratios for axisymmetric and three-dimensional solutions are plotted, not shown here. To do so, we have assumed that vortex tube is used to cool a piece at ambient temperature (assumed 27 °C). Power of cooling for a vortex tube is defined as $\dot{Q}_c \quad \dot{m}_c\, c_p(T_{oA} - T_{oc})$ where $\dot{m}_c$ is the cold outlet mass flow rate, c_p – the specific heat at constant pressure, T_{oA} – the total temperature of ambient assumed equal to the static temperature of the ambient, and T_{oc} – the total cold outlet temperature. We see that in a designed cold temperature, two-dimensional axisymmetric model gives more power of cooling than three-dimensional model. For example, maximum difference is 131% that occurs for the case $\dot{m}_{in}$ = 8.35 g/s, T_{oin} = 300 K, and P_h/P_c = = 1.78 and minimum difference is 29% that occurs for the case $\dot{m}_{in}$ = 8.35 g/s, T_{oin} = 300 K, and P_h/P_c = 1.3. So, designing with the results of two-dimensional model will not be accurate and may lead to the failure of the piece. Moreover, this figures show that lowering the cold outlet temperature does not necessarily results in higher power of cooling, because mass flow rate also contribute to the power of cooling.

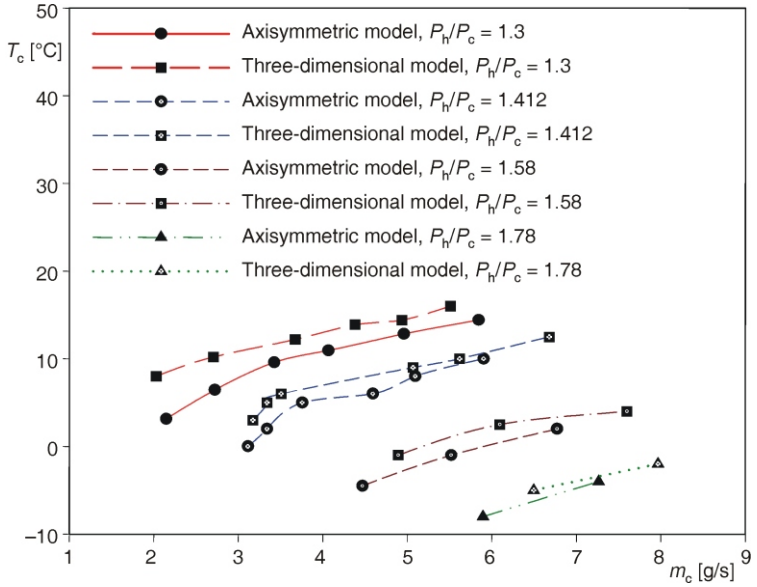

Figure 21. Variation of cold outlet temperature *vs*. cold mass flow rate in different pressure ratios for axisymmetric and three-dimensional solutions for a two nozzle vortex tube for the case $\dot{m}_{in}$ = 8.35 g/s and T_{oin} = 300 K

Conclusions

In this work using two-dimensional axisymmetric and three-dimensional numerical models, mechanisms of flow and heat transfer in a two-nozzles vortex tube were analysed. It was concluded that both transfer of shear work because of radial gradient of tangential velocity from core region to the outer region, and change of mean kinetic energy between the core region with higher kinetic energy and near wall region with lower kinetic energy contribute significantly in generating energy separation in the vortex tube.

It was also shown that using three-dimensional numerical model gives more accurate results compared to two-dimensional axisymmetric numerical model. These results were confirmed by comparing them with available experimental data. In addition, non-dimensional analysis was performed to achieve effective non-dimensional parameters to be used for presenting the numerical results. In order to understand the physics of the problem some dimensional plots describing the power of cooling at different cold outlet temperatures were presented. These results showed that axisymmetric model overestimates power of cooling compared to three-dimensional numerical model.

References

[1] Ranque, M.G., Experiments on Expansion in a Vortex with Simultaneous Exhaust of Hot Air and Cold Air, (in French), *J Phys Radium, 7* (1933), 4, pp.112-114
[2] Hilsh, R., The Use of Expansion of Gases In Centrifugal Field as a Cooling Process, *Rew Sci. Instrum, 18* (1947), 2, pp. 108-113
[3] Eiamsa, S., Promvonge, P., Numerical Investigation of the Thermal Separation in Ranque – Hilsh Vortex tube, *Int. J. Heat Mass Transfer, 50* (2007), 5-6, pp. 821-832
[4] Aljuwayhel, N. F., Nellis, G. F., Parametric and Internal Study of the Vortex Tube Using CFD Model, *Int. J. Refrigeration, 28* (2005), 3, pp. 442-450
[5] Farouk, T., Farouk, B., Large Eddy Simulations of the Flow Field and Temperature Separation in the Ranque – Hilsch Vortex Tube, *Int. J. Heat and Mass Transfer, 50* (2007), 23, pp. 4724-4735
[6] Aydin, O., Baki, M., An Experimental Study on the Design Parameters of a Counter Flow Vortex Tube, *Energy, 31*(2006), 14, pp. 2763-2772
[7] Frohlingsdorf, W., Unger, H., Numerical Investigation of the Compressible Flow and Energy Separation in Ranque-Hilsh Vortex Tube, *Int. J. Heat Mass Transfer, 42* (1999), 3, pp. 415-422
[8] Behera, U., *et al*., CFD Analysis and Experimental Investigations Towards Optimizing the Parameters of Ranque-Hilsh Vortex Tube, *Int. J. Heat Mass Transfer, 48* (2005), 10, pp. 1961-1973
[9] Skye, H. M., Nellis, G. F., Comparison of CFD Analysis to Empirical Data in Commercial Vortex Tube, *Int. J. Refrigeration, 29* (2006), 1, pp. 71-80
[10] Eiamsa-ard, S., Promvonge, P., Investigation on the Vortex Thermal Separation in a Vortex Tube Refrigerator, *Science Asia, 31* (2005), 3, pp. 215-223
[11] Hartnett, J. P., Eckert, E., Experimental Study of the Velocity and Temperature Distribution in a High-Velocity Vortex-Type Flow, *Trans. ASME J. Heat Transfer, 79* (1957), 4, pp.751–759
[12] Eiamsa-ard, S., Promvonge, P., Review of Ranque–Hilsch Effects in Vortex Tubes, *Renewable and Sustainable Energy Reviews, 12* (2008), 7, pp. 1822-1842
[13] Aljuwayhel, N. F., Internal Study of Vortex Tube Using a CFD Package, M. Sc. thesis, University of Wisconsin-Madison, Vis., USA, 2003

Authors´ affiliation:

A. Hossein Nezhad (**corresponding author**)
Department of Mechanical Engineering, University of Sistan and Baluchestan,
Zahedan, Iran
Postal code: 98135-987
E-mail: nezhadd@hamoon.usb.ac.ir

R. Shamsoddini
Department of Mechanical Engineering, University of Sistan and Baluchestan,
Zahedan, Iran

Paper submitted: August 12, 2008
Paper revised: November 11, 2008
Paper accepted: December 27, 2008